Journal of Applied Polymer Science

Electrosynthesis of poly(3-amino-4-hydroxybenzoic acid) nanoparticles with electroactivity even in highly alkaline solutions

Chuanxiang Chen, Xiaozhang Hong, Yuhua Gao
Department of Chemistry and Chemical Engineering, School of Environmental and Chemical Engineering, Jiangsu University of Science and Technology, Zhenjiang 212003, People's Republic of China
Correspondence to: C. Chen (E-mail: cxchen@just.edu.cn)

ABSTRACT: Electroactive poly(3-amino-4-hydroxybenzoic acid) nanoparticles were synthesized using cyclic voltammetry and exhibited high electroactivity in 0.30 M Na_2SO_4 solutions with pH values ranging from 1.0 to 12.0. This indicates that polymer has excellent electrochemical properties even in near-neutral and alkaline solutions compared to polyaniline. The anodic and cathodic peak currents of the polymer increase linearly with the square root of scan rate from 5 to 150 mV s^{-1}, indicating that the electrode reaction is controlled by a diffusion process. The structure of the polymer was investigated using UV–visible spectroscopy, Fourier transform infrared spectroscopy, proton nuclear magnetic resonance, and X-ray photoelectron spectroscopy. Based on the spectroscopic measurements, a possible polymerization mechanism of 3-amino-4-hydroxybenzoic acid was proposed. The polymer surface morphology was characterized by scanning electron microscopy. The enhanced electrochemical properties are ascribed to the synergistic effect of —COOH and —OH groups in the polymer chains. © 2015 Wiley Periodicals, Inc. J. Appl. Polym. Sci. **2015**, *132*, 42190.

KEYWORDS: electrochemistry; FTIR; synthesis

Received 25 October 2014; accepted 13 March 2015
DOI: 10.1002/app.42190

INTRODUCTION

Conducting polymers have been intensively studied during the past three and a half decades, because of their numerous technological applications.[1–3] Polyaniline is one of the most widely studied conducting polymers due to its facile synthesis, excellent chemical and environmental stability, good electrical conductivity, and great potential for advanced applications in lightweight battery electrodes, anticorrosion coatings, chemical sensors, biosensors, and optical and electronic devices.[4–7]

Nanostructures of polyaniline have attracted growing attention because they display new interesting properties arising from their nanoscale sizes, and have greatly improved performance in devices.[8–11] For example, in sensor applications, polyaniline nanofibers exhibit much higher sensitivity and faster time response in contrast to the conventional bulk counterparts because of higher effective interfacial area and shorter penetration depth for target molecules.[12,13]

Several methods, which include electrospinning, chemical polymerization, and electrochemical polymerization, have been used for preparing the nanostructures of polyaniline.[14–16] The conventional chemical polymerization can be used to make bulk quantities of nanostructured polyaniline with the aid of insoluble templates, soluble templates, or biological templates. Recently, the interfacial chemical polymerization has been considered as another general method to prepare bulk quantities of polyaniline nanostructures in the absence of any template.[13] However, the electrochemical polymerization has still received considerable attention due to relatively easy controllability of experimental conditions compared to the conventional or interfacial chemical polymerization. Moreover, the polyaniline nanostructures can be obtained directly on conductive substrates *via* the electrochemical polymerization, and it is therefore convenient to study their electrochemical properties. Some recent work indicates that the pure polyaniline nanowires can be made without requiring any template by simply controlling the electrochemical polymerization kinetics.[17] However, in spite of the variety of preparation methods reported, polyaniline derivative nanostructures have been prepared with only limited success so far.[18]

Many interesting researches have focused on the polyaniline derivatives prepared in different ways due to enhanced properties compared to the parent polymer.[2,5,19] One way is to polymerize substituted anilines. Most of the polymers obtained from substituted anilines such as *N*-alkylanilines are soluble in common organic solvents and they are therefore easily processable.[20] Moreover, the structural, redox, and electrochemical properties of the polymers formed from substituted anilines are

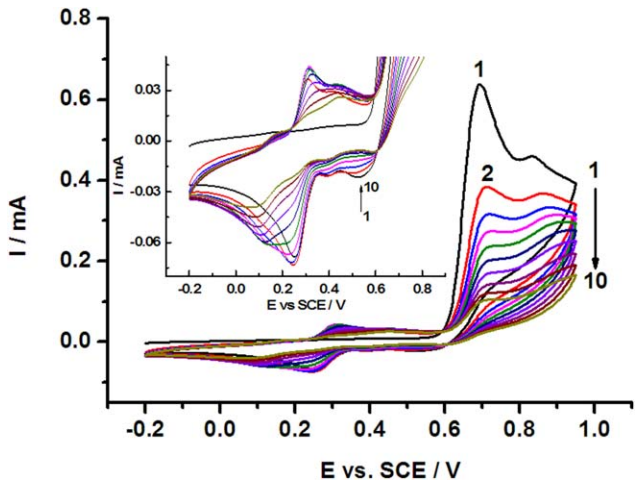

Figure 1. Consecutive cyclic voltammograms of polymerization of AHBA at the potential range of −0.20 to 0.95 V in 0.02 M AHBA and 0.50 M H_2SO_4 solution. Scan rate: 100 mV s^{-1}. The number of curves in the plot corresponds to the number of cycles. [Color figure can be viewed in the online issue, which is available at wileyonlinelibrary.com.]

either quite similar to that of polyaniline[21–23] or apparently different.[2,24,25] This, therefore, offers the possibilities of enhanced performance in various technological applications.

Recently, Kan *et al.* reported that the electrochemical oxidation of 3-amino-4-hydroxybenzoic acid (AHBA), an aniline derivative, was carried out at a platinum electrode in an aqueous HCl solution at constant potential (1.5 V).[26] However, they only studied the solubility in polar solvents, conductivity (2.3×10^{-4} S cm^{-1}), and solvatochromism of the resulting novel polymer. Chen *et al.* reported the electrochemical copolymerization of aniline with 3-amino-4-hydroxybenzoic acid using cyclic voltammetry.[25] The copolymer has a good electroactivity at pH ≤11. The pH dependence of the electroactivity of the copolymer is better than that of the unsubstituted polyaniline. This is mainly attributed to two pH functional groups of —OH and —COOH in the 3-amino-4-hydroxybenzoic acid unit in the copolymer backbone. To date, there are no electrochemical properties, formation mechanism, and UV–visible, X-ray photoelectron spectroscopy (XPS), and proton nuclear magnetic resonance (^{1}H NMR) spectra of the polymer, which limits the further applications of this novel conducting polymer, poly(3-amino-4-hydroxybenzoic) (PAHBA).

At present, among many electrochemical methods used in the study of chemical reactions, cyclic voltammetry is a very popular technique for initial electrochemical studies of new systems and is used widely to obtain information on complicated electrode reactions. In this study, cyclic voltammetry was used to perform the polymerization of AHBA at a glassy carbon electrode in an aqueous sulfuric acid solution. AHBA has two functional groups (—NH_2 and —OH), which could be electrochemically oxidized to form active species for polymerization. In addition, it contains two acidic functional groups (—COOH and —OH), which would affect the properties of the resulting polymer.

EXPERIMENTAL

Materials

All chemicals were supplied by Sigma-Aldrich Chemicals Inc. (USA) and used without further purification. Aqueous solutions were prepared using ultrapure water (Milli-Q, Millipore).

Electrochemical Synthesis

Electrochemical synthesis was carried out using a traditional three-electrode cell. A glassy carbon (GC, 3 mm diameter) or an indium-tin oxide (ITO, 7 mm × 25 mm) conducting glass was used as a working electrode, and a platinum foil severed as an auxiliary electrode. A saturated calomel electrode was used as a reference electrode. All potentials in this work are given against this reference. Prior to each electrochemical synthesis, the GC electrode was polished with 0.3 μm alumina slurry, then rinsed with distilled water, and finally sonicated in distilled water for 10 min. All electrochemical experiments were performed using a potentiostat/galvanostat Autolab PGSTAT 30 (Eco Chemie, The Netherlands) at room temperature.

The polymerization rate of a monomer and the property of the resulting polymer are generally affected by many factors. In this work, we mainly discuss the influence of switching potential window on the polymerization of AHBA. Poly(3-amino-4-hydroxybenzoic acid) (PAHBA) film was prepared using cyclic voltammetry in 0.02 M AHBA and 0.50 M H_2SO_4 solution. The scan rate was set at 100 mV s^{-1}. The scan potential range was controlled from −0.20 to 0.95 V or between −0.20 and 0.80 V. All the polymer electrodes obtained were rinsed using ultrapure water to remove adsorbed AHBA and oligomers on the electrode surfaces.

Characterizations

Cyclic voltammetry of polymer films was performed using the potentiostat/galvanostat Autolab PGSTAT 30 (Eco Chemie, The Netherlands) in 0.50 M H_2SO_4, and then in 0.50 M Na_2SO_4 solutions with pH ranging from 1.0 to 12.0. The 0.30 M Na_2SO_4 solutions with various pH values were adjusted by adding

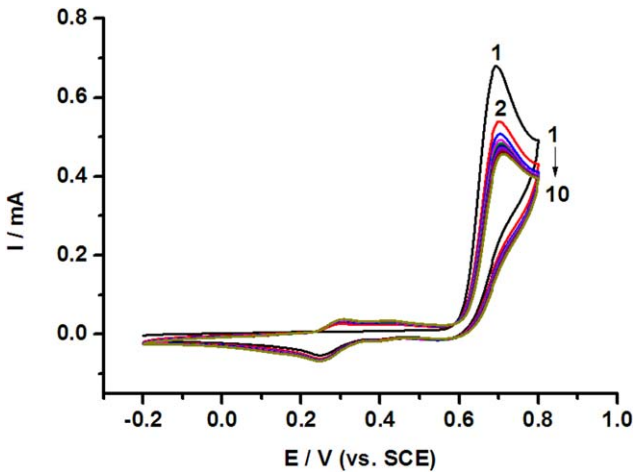

Figure 2. Consecutive cyclic voltammograms of polymerization of AHBA at the potential range of −0.20 to 0.80 V in 0.02 M AHBA and 0.50 M H_2SO_4 solution. Scan rate: 100 mV s^{-1}. The number of curves in the plot corresponds to the number of cycles. [Color figure can be viewed in the online issue, which is available at wileyonlinelibrary.com.]

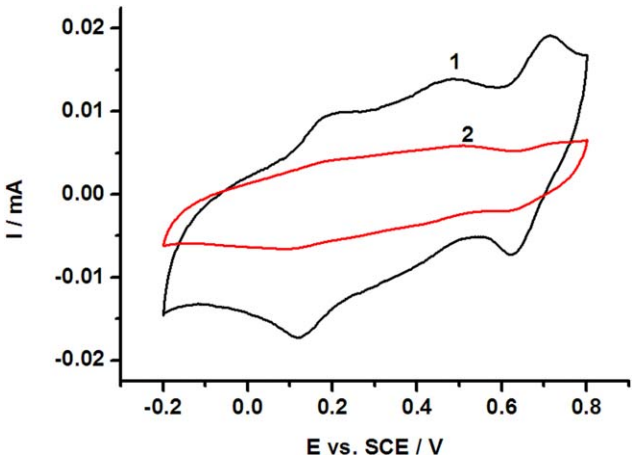

Figure 3. Cyclic voltammograms of the polymers in 0.5 M H_2SO_4, Scan rate: 100 mV s^{-1}. The polymers were synthesized under the same conditions used for Figure 1, except for different potential ranges, curves: (1) $-0.20 \sim 0.95$ V and (2) $-0.20 \sim 0.80$ V. [Color figure can be viewed in the online issue, which is available at wileyonlinelibrary.com.]

concentrated NaOH or H_2SO_4 to achieve the desired pH which was determined by a model EL20 Education Line pH meter (Mettler-Toledo, USA).

The UV–visible absorptive spectra of the dried AHBA thin film on an ITO plate and PAHBA film electrosynthesized on an ITO electrode was performed on a UV-2501PC spectrometer (Shimadzu, Japan). The Fourier transform infrared (FTIR) spectra of the dried AHBA and PAHBA were collected on a Frontier Fourier transform infrared spectrometer (PerkinElmer, USA) using attenuated total reflection technique. ^{1}H NMR spectra were recorded at 600 MHz on an Avance 600 NMR spectrometer (Bruker, Germany) at 303.1 K. Each sample was dissolved in deuterateddimethyl sulfoxide (DMSO-d_6) in an NMR tube and tetramethylsilane (TMS) was used as an internal reference. XPS measurements were performed on an ESCALab 250 spectrometer (Thermo VG Scientific, USA) using an Al K_α radiation (1486.6 eV), and all the binding energies were referenced to the C 1s peak at 284.8 eV arising from the surface adventitious carbon. The surface morphology of the polymer film was observed in a JSM-6340F scanning electron microscopy (SEM) (JEOL, Japan) at an acceleration voltage of 10 kV. Before analysis, the surface of each sample was sputter-coated with platinum.

RESULTS AND DISCUSSION

Electrochemical Polymerization of AHBA

The electrochemical polymerization of AHBA was studied in a 0.50 M H_2SO_4 aqueous solution on a GC electrode at 35°C. Unless otherwise stated, this is the solvent/electrolyte system and temperature used throughout this work.

Typical cyclic voltammograms of AHBA are shown in Figure 1, where the electrode potential was swept continuously at a rate of 100 mV s^{-1} between -0.2 and 0.95 V. As can be observed from the first potential scan, there are two oxidation peaks at 0.69 and 0.89 V. On the negative sweep, none of these peaks show corresponding reduction peaks. According to the previous research results concerning the electrochemical oxidations of aromatic compounds with —NH_2 and —OH groups,[27–30] the first anodic peak could be attributed to the fact that the adsorbed protonated AHBA is oxidized to the monocation radical, and the second one could be ascribed to the fact that the two monocations absorbed on the electrode surface further are oxidized to the dimer. The dimer can be oxidized and then further react with one AHBA radical to form a trimer. Such successive reactions lead to the formation of PAHBA on the working electrode. In the second potential scan, the two oxidation peak currents of the monomer decrease significantly. This is due to that the —COOH electron-withdrawing group lowers the electron density on the amino group, and the —OH electron-donating group acts as a amino radical scavenger. However, the oxidization behavior of AHBA is associated with the generation of a polymer on the surface of the GC electrode. The oxidization peak currents of AHBA become smaller, but the polymerization continues because the surface of the working electrode is not fully covered by PAHBA in the first cycle. Therefore, the AHBA molecules can continue to be oxidized to form the polymer in the second and subsequent potential scan cycles. In addition, the potentials of the two oxidization peaks shift toward more positive potentials with an increase in the number of potential scan cycles. These results indicate that the polymer has a low conductivity. The evidence for this is that a reddish brown film was observed at the working electrode and the solution around the working electrode became brown, indicating that the polymer partially dissolved in the aqueous solution. This result is similar to the electrochemical polymerization behavior of 5-aminosalicylic acid.[31]

Besides that, a cathodic peak occurs at about 0.25 V on curve 1. Two anodic peaks at about 0.31 and 0.42 V and their corresponding cathodic peaks appear at about 0.39 and 0.24 V for the second cycle (curve 2). Three anodic peaks occur at about 0.17, 0.31, and 0.42 V and their corresponding cathodic peaks appear at about 0.13, 0.24, and 0.40 V for the third cycle (curve 3). In the following potential scan, the three redox pairs still occur in the potential range of -0.20 to 0.50 V. However, the

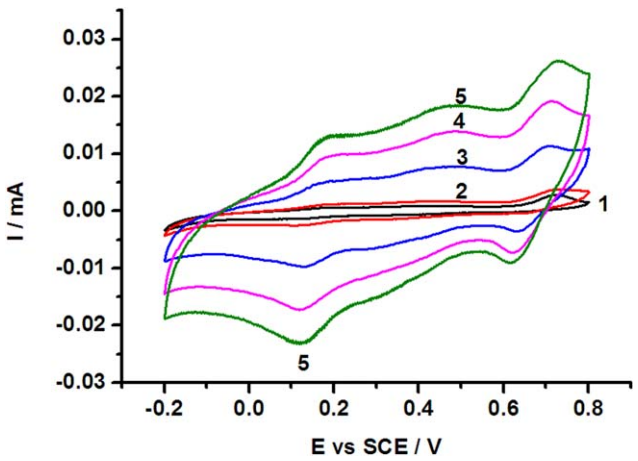

Figure 4. Effect of potential scan rate on the cyclic voltammetry of PAHBA in a solution of 0.5 M H_2SO_4. Scan rates: (1) 5, (2) 10, (3) 5, (4) 100, and (5) 150 mV s^{-1}. [Color figure can be viewed in the online issue, which is available at wileyonlinelibrary.com.]

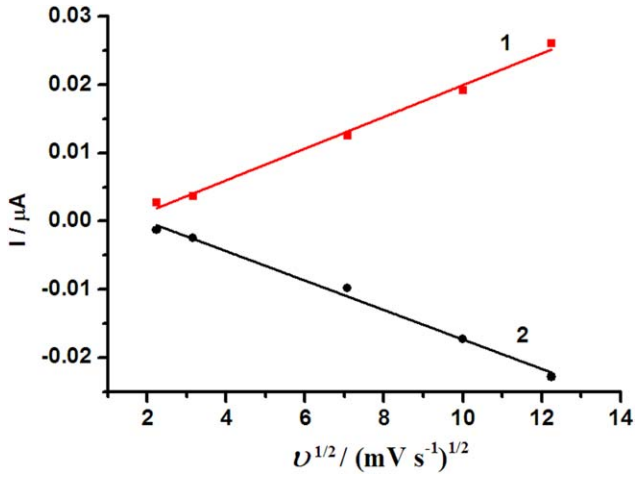

Figure 5. Plots of the maximum (1) anodic peak current and (2) cathodic peak current versus $\upsilon^{1/2}$ based on the data in Figure 4. [Color figure can be viewed in the online issue, which is available at wileyonlinelibrary.com.]

three anodic peaks appear at about 0.17, 0.31, and 0.45 V and their corresponding cathodic peaks occur at about 0.06, 0.24, and 0.40 V for the tenth cycle (curve 10). Based on the result concerning the electrochemical polymerization of *o*-aminophenol,[27] a redox pair at 0.31/0.24 V may be assigned to the dimers oxidize to the corresponding dications at lower potentials than AHBA. Another two pairs of the redox peaks at lower potentials arise from the redox of the polymer itself. After the completion of 10 cycles, the polymer electrode was thoroughly rinsed using ultrapure water to remove adsorbed AHBA on the electrode surface before use in the following characterization experiments. This purification is enough to evaluate the structure and electrochemical properties of the resulting polymer.

The upper potential scan limit is important for the formation of polyaniline and its derivatives. Figure 2 shows the cyclic voltammograms of AHBA under the same conditions as shown in Figure 1, but the upper potential scan limit is 0.80 V. It is clear that the polymerization rate in Figure 2 is much slower than that in Figure 1. This reveals that it is unfavorable to the formation of PAHBA in the same condition with decreasing the switching potential. However, after electrolysis, a thin polymer film was also obtained on the working electrode. The thin polymer film modified electrode was thoroughly rinsed with ultrapure water and then used for the electrochemical experiment.

Electrochemical Properties of the Polymers

Curves 1 and 2 in Figure 3, respectively, are the cyclic voltammograms of the polymer films obtained from Figures 1 and 2 in 0.50 M H_2SO_4 solution. As can be seen in Figure 3, three anodic and two cathodic waves occur on curves 1 and 2, which are very similar in shape. This indicates that electrochemical activity of both polymer films is somewhat similar in the acid solution. However, based on the areas of curves 1 and 2, the polymer film obtained in Figure 1 has much higher electrochemical activity than that in Figure 2. This is mainly due to that the hydroxyl group of AHBA inhibited the polymerization of AHBA during electrolysis and that a low upper switching potential was not favorable to the polymer growth. Therefore, the polymer film obtained in the potential range of −0.20 to 0.95 V in Figure 1 was used in the following characterization experiments, unless otherwise stated.

Figure 4 shows the cyclic voltammograms of PAHBA in 0.50 M H_2SO_4 at different scan rates between 5 and 150 mV s^{-1}. It is evident that their peak currents increase with potential scan rates, and that all the peak potentials are independent of potential scan rate in the above scan rate range. There are still three anodic peaks and two sharp cathodic peaks at 150 mV s^{-1} on curve 5, indicating that the electrochemical reaction is still controlled by mass transfer at this scan rate. Based on the relationship between the potential scan rate υ and the maximum anodic (cathodic) peak current, the maximum peak currents varied linearly with $\upsilon^{1/2}$ (Figure 5). This again proves that the electrode reaction of PAHBA is controlled by mass transfer.

In order to gain further insights into the electrochemical activity of the polymer, its cyclic voltammetry was determined in 0.30 M Na_2SO_4 solutions with pH values from 1.0 to 12.0

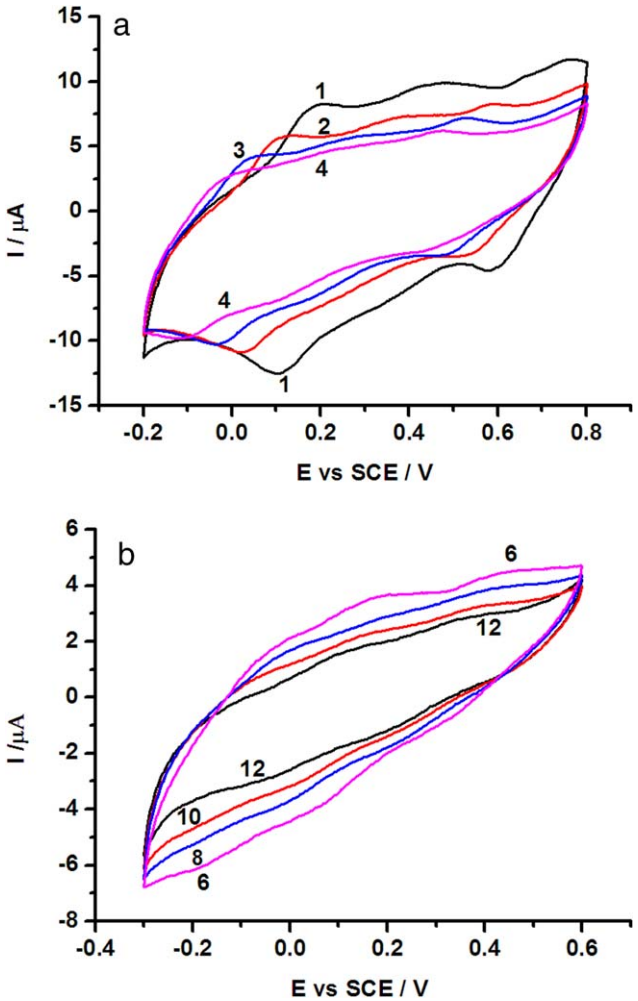

Figure 6. Cyclic voltammograms of PAHBA in 0.30 M Na_2SO_4 with various pH values. The number of curves in the plot corresponds to the pH value. [Color figure can be viewed in the online issue, which is available at wileyonlinelibrary.com.]

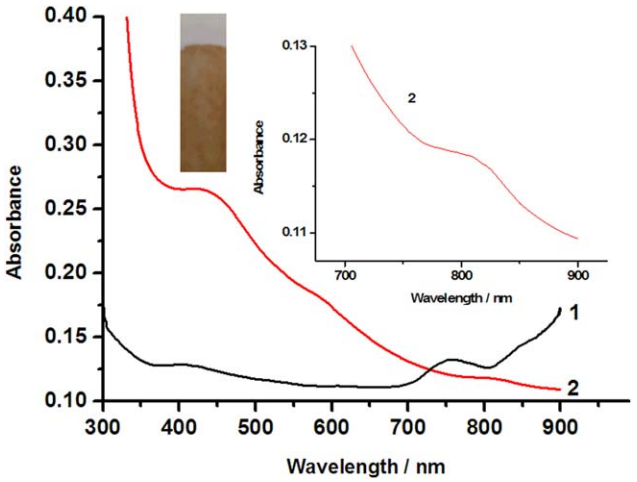

Figure 7. UV–visible spectra of (1) AHBA monomer film and (2) PAHBA thin film on ITO glass electrode. The inset picture is the PAHBA film. [Color figure can be viewed in the online issue, which is available at wileyonlinelibrary.com.]

(Figure 6). As can be seen in Figure 6(A), there are three anodic and two cathodic waves occur on curve 1. All the anodic and two cathodic waves shift slowly toward more positive potentials and more negative potentials, respectively, with the increasing pH values. This reveals that the redox processes of the polymer are related to proton concentration of the solution, i.e., protons in the polymer release into the solution for the oxidation process, and vice versa for the reduction process. Generally, phenols can be oxidized to quinones and the quinones can be reduced reversibly. Therefore, the redox couple situated at most positive potentials could be ascribed to the redox reaction of phenolic —OH groups in the PAHBA, i.e., the electron transfer is coupled with proton exchange between the polymer and the solution. This result is in agreement with the curve 10 in Figure 1 since there is a redox couple at about 0.65 V. The anodic peak in Figure 1 is assigned to the oxidization of phenolic —OH groups. In fact, there is a new cathodic peak at about 0.60 V for the tenth cycle in Figure 1. This redox wave is due to that the —OH group in the polymer chain can be reversibly oxidized and reduced. This redox wave is attributed to that the —OH group in the polymer chain can be reversibly oxidized and reduced. Based on the result reported by Mu[32] that there are a redox wave at 0.16/0.08 V and an oxidization peak at 0.60 V on the cyclic voltammetry of poly(o-aminophenol) in 0.30 M H_2SO_4 solution, the redox wave at most negative potentials could be ascribed to the nonprotonization and protonization of imino (—NH—) groups of oxidized PAHBA. The anodic peak at more positive potentials could be attributed to the doping of ionized carboxylic acid ($—COO^-$) groups of the polymer. Both the —NH— and $—COO^-$ groups are nonprotonized and their protonization degree decrease with increasing solution pH.

In addition, the redox peak currents in Figure 6(B) decrease very slowly with increasing the pH values from 6.0 to 12.0. This indicates a slow decay in the electrochemical activity of the polymer with pH in the above pH range. Based on the areas of curves 6 and 12, the polymer shows a 44.5% decrease in the electrochemical activity when it was transferred from pH 6.0 to 12.0. This means that the polymer still hold a good electrochemical property in the aqueous solution of pH 12.0. It is obvious that the polymer has higher electrochemical activity than that of the unsubstituted polyaniline.[33] This is attributed to the synergistic effect of the —COOH and —OH functional groups in the polymer chain. The presence of —COOH groups provides the high concentration of protons in the polymer backbone, which results not only in improving the redox behavior but also in enhancing the charge-transfer rate at higher pH values. The phonic —OH functional groups can be oxidized and reduced reversibly, which also plays a key role in adjusting the pH value to around the electrode and enhancing the redox activity.

UV–Visible Spectra

Curves 1 and 2 in Figure 7 show the UV–visible spectra of the dried AHBA thin film-ITO and PAHB-modified ITO,

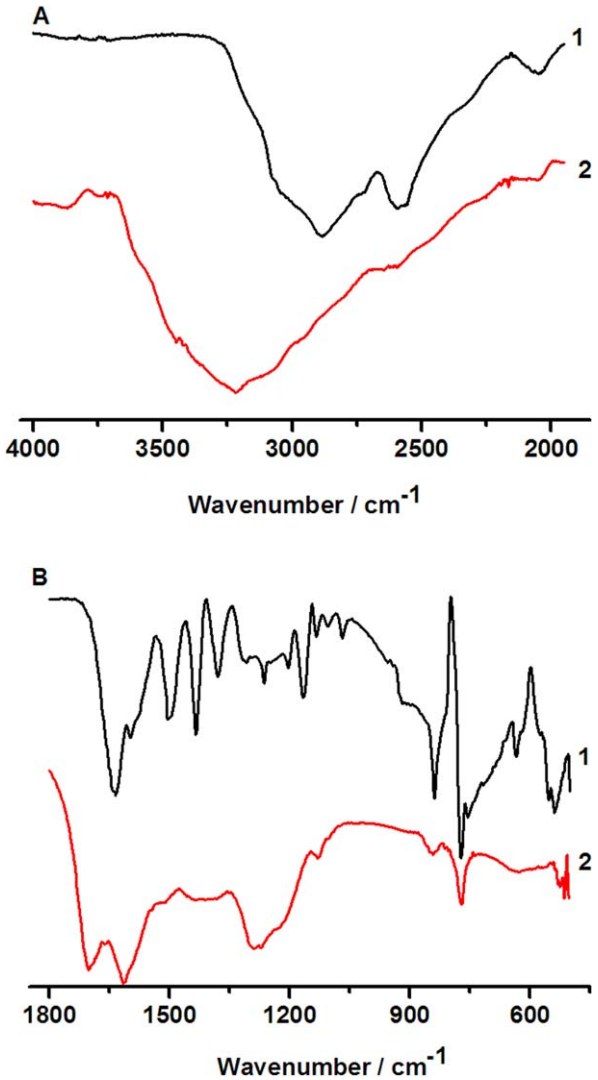

Figure 8. FTIR spectra in the wavenumber regions of (A) 4000 ~ 2000 cm^{-1} and (B) 1800 ~ 500 cm^{-1} for (1) AHBA and (2) PAHBA. [Color figure can be viewed in the online issue, which is available at wileyonlinelibrary.com.]

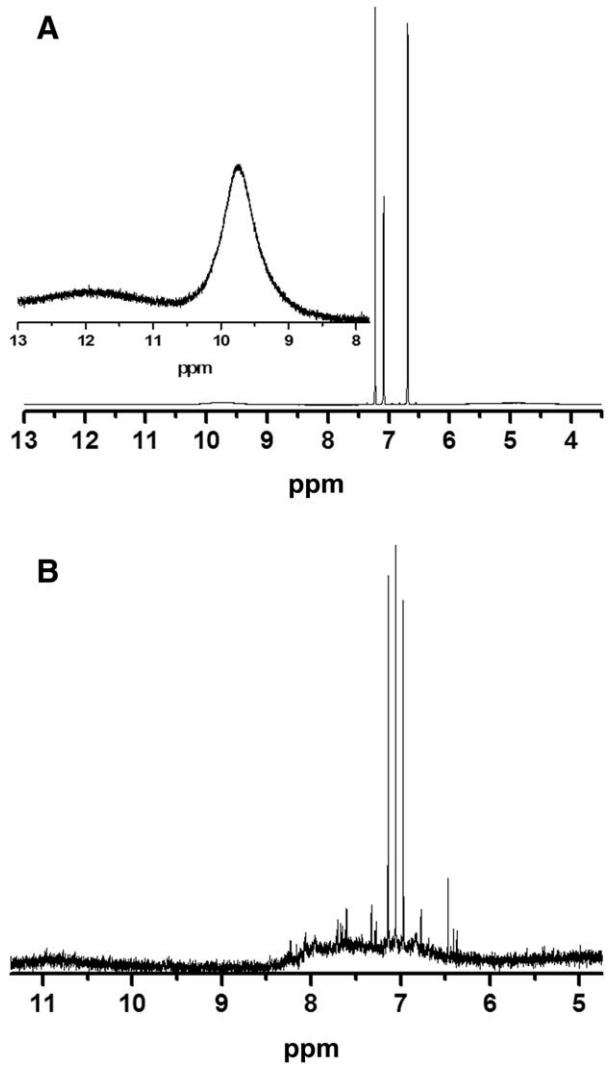

Figure 9. ^{1}H NMR spectra of (A) AHBA and (B) PAHBA.

respectively. The AHBA monomer thin film was prepared by drop-casting aqueous AHBA solution on an ITO plate, and dried in a dry nitrogen stream. PAHBA thin film was deposited on the ITO glass electrode under the same condition of Figure 1 except for the working electrode material. The inset picture in Figure 7 shows the electrodeposition of the yellow-brown PAHBA film. The conductivity of PAHBA obtained here is 1.7 $\times$ 10^{-5} S cm^{-1}, which is much lower than that of the green PAHBA electrosynthesized on a platinum electrode in an aqueous HCl solution at constant potential (1.5 V).[26] As can be seen in Figure 7, two signals of the monomer at 405 and 758 nm appear in curve 2 but are shifted to 439 and 817 nm. This is due to conjugation in the PAHBA backbone. The two peaks of the polymer may originate from the charged cationic species known as polarons, similar to those of polyaniline.[34] In addition, it should be noted that there is a new shoulder peak at about 585 nm in curve 2. This is similar to that of the emeraldine base form of polyaniline, which has a typical visible absorption peak at 570 nm.[35] Based on the fact that AHBA is an aniline derivative, it is thus expected that the chemical structure of PAHBA here could be similar to that of polyaniline.

FTIR Spectra

Figure 8 shows the FTIR spectra of the (1) AHBA monomer and (2) PAHBA film. The IR spectrum of the PAHBA film obtained here is different from that of the polymer, poly(2,5-benzoxazole), prepared *via* chemical polymerization of 3-amino-4-hydroxybenzoic acid hydrochloride, in a mildly acidic poly(phosphoric acid) medium, in which the O—H stretching vibration peak at about 3400 cm^{-1} appeared, but the carboxylic C=O stretching vibration band at about 1710 cm^{-1} disappeared.[36] This demonstrates that the polymer formed here is not poly(2,5-benzoxazole) but a new material. In addition, the spectrum of PAHBA obtained here is different from that of the polymer electrosynthesized at a platinum electrode in an aqueous HCl solution at constant potential,[26] because the strong absorption peak at 1550 cm^{-1} appears in the latter while it does not occur in the former. In curve 1, the shoulder peak observed at 3052 cm^{-1} is assigned to the C—H stretching vibration, while the broad bands observed in the range of 2000 $\sim$ 3000 cm^{-1} are attributed to the O—H stretching vibration arising from intramolecular hydrogen bonding between the hydroxylic H atom and the carboxylic oxygen atom. The strong peak at 1633 cm^{-1} is assigned to the C=O stretching and $-NH_2$ scissors[37,38] vibrations. The peak at 1597 cm^{-1} is mainly attributed to the $-NH_2$ scissors vibration mixed by the aromatic ring C=C vibrations.[38] The peak at 1506 cm^{-1} is ascribed to the aromatic ring C=C vibration.[39] The peak at 1434 cm^{-1} is due to aromatic ring C=C stretching and in-plane —OH bending vibrations.[37] The peak at 1385 cm^{-1} is mainly attributed to the carboxylic O—H stretching vibration. The two peaks at 1312 and 1264 cm^{-1} are assigned to the C—N stretching and/or phenolic O—H stretching vibrations. The peak at 1209 cm^{-1} is attributed to the phenolic C—O stretching and C—H stretching vibrations. The peak at 1166 cm^{-1} is attributed to the $-NH_2$ twist[37] and carboxylic O—H out-of-plane bending and C—H stretching vibrations.[38] The two weak peaks at 1105 and 1069 cm^{-1} are attributed to the C—H in-plane bending vibration. The two strong peaks at 839 and 770 cm^{-1} are attributed to the C—H out-of-plane bending vibration. The peak at 633 cm^{-1} is assigned to the phenolic O—H out-of-plane bending vibration, respectively. The peak at 533 cm^{-1} is attributed to the out-of-plane ring deformation.

In curve 2, the broad band centered near 3215 cm^{-1} is attributed to the N—H stretching vibrations of the secondary aromatic amine, coupled with the phenolic and carboxylic O—H stretching vibrations. This means that the transformation of a primary to a secondary amine and coupling occurred through the amino groups and there are free —OH groups in the polymer chain. The strong carboxylic C=O stretching vibration peak at 1701 cm^{-1} occurs in curve 2, indicating that carboxylic groups still present in the polymer chain. The strong new peak at 1610 cm^{-1}, attributed to the N—H stretching vibration of the secondary aromatic amine, appears in curve 2, and the monomer peak at 1597 cm^{-1}, mainly to $-NH_2$ scissors vibration, disappears in the polymer spectrum. However, there are two weak quinone and benzenoid C=C stretching vibration peaks at 1501 and 1435 cm^{-1}, respectively, occur in curve 2, indicating that the phenyl rings are not broken. The broad and weak peaks around 1380 cm^{-1}, corresponding to the carboxylic

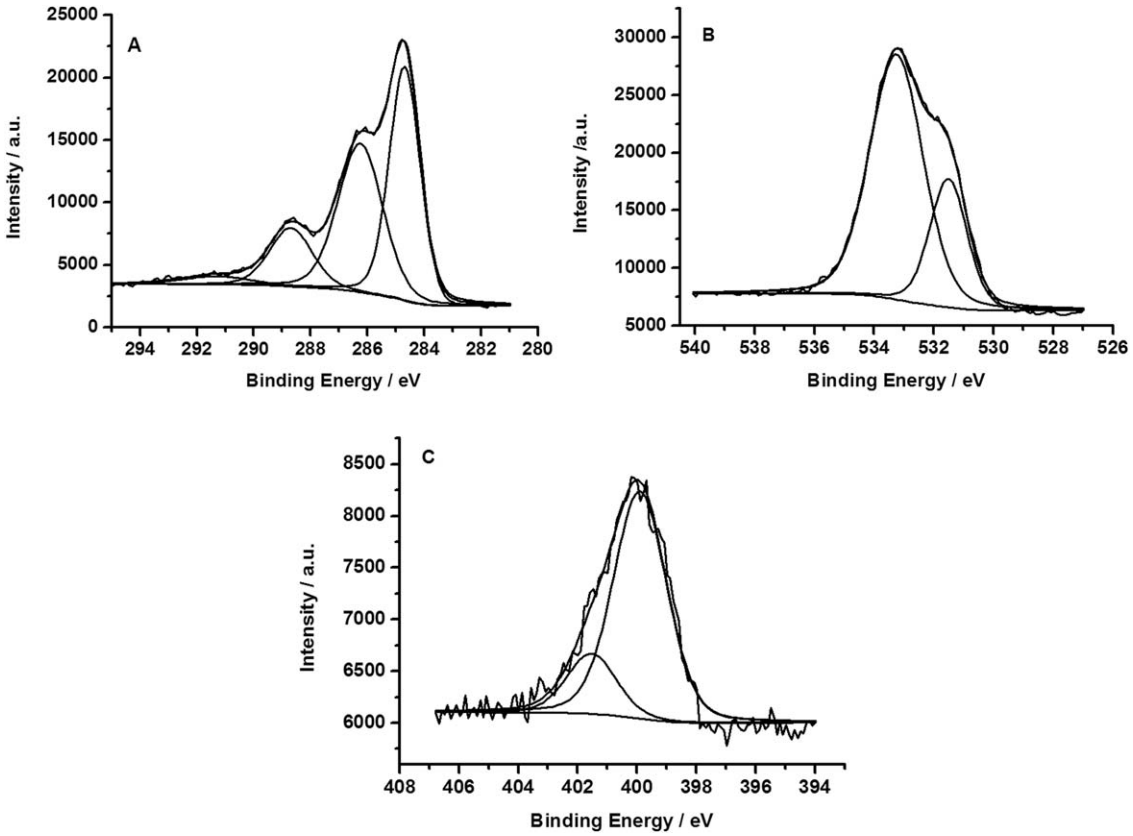

Figure 10. (A) C 1s, (B) O 1s, and (C) N 1s high-resolution XPS spectra for the PAHBA film.

O—H stretching vibration, appears in curve 2. This further proves that there are carboxylic groups in the polymer chain. The peaks at 1285 and 1271 cm^{-1} are mainly ascribed to the C—N stretching and/or phenolic O—H stretching vibrations, but the intensities of the two peaks become strong. This means there are more C—N bonds in the polymer chain than the monomer, i.e., —NH_2 groups of AHBA took part in formation of the polymer main chain. The peak at 630 cm^{-1} is attributed to the phenolic O—H in-plane and out-of-plane bending vibrations,[40] which further proves the presence of free phenolic —OH groups in the polymer chain. The two aromatic C—H out-of-plane bending vibration peaks at 840 and 770 cm^{-1} observed in curve 1 appear in curve 2, but the intensities of the two peaks become weak. In addition, the S=O stretching vibration peak at 1129 cm^{-1} occurs in curve 2, which demonstrates that SO_4^{2-} ions were doped into the polymer during the polymerization in the sulfuric acid solution. However, the intensity of the peak is very weak, which reveals just a few SO_4^{2-} ions were incorporated into the polymer chain. As a result, the conductance of the PAHBA film is rather poor, which led to a decrease in the AHBA polymerization rate with an increasing number of scanning cycles. The above results demonstrate that the IR spectrum of the polymer film is different from that of AHBA. This means that an electrochemical polymerization of AHBA took place in this work.

Table I. XPS Experimental Results of C 1s in the PAHBA Film

Binding energy (eV)	Area	At % (determined)	At % (calculated)
284.7	27,444	42.9	42.9
286.3	25,122	39.2	42.9
288.7	9451	14.8	14.2
291.4	2001	3.1	

It is important to notice the absence of the characteristic absorptions of the C—O—C group (1070 cm^{-1})[29] and phenoxazine-type unit (575 cm^{-1})[41] in the polymer spectra. The absence of both indicates that the polymer is a linear rather than ladder phenoxazine-like chain structure and in the linear form, phenolic —OH groups are free. In addition, the polymer structure obtained here is completely different from that prepared through the polycondensation reaction in the mildly acidic poly(phosphoric acid) medium, where all the —COOH, —OH, and —NH_2 groups of AHBA took part in the formation of the complete oxazole rings *via* the complete cyclization reaction.[36]

^{1}H NMR Spectra

Figure 9(A) shows the ^{1}H NMR spectrum of AHBA. A broad peak at 4.90 ppm is attributed to the —NH_2 proton resonance.[42] Three sharp signals at 6.70, 7.10, and 7.23 ppm are caused by the three aromatic protons on the *ortho* position of the —OH group, and the *para* and *ortho* positions of the —NH_2 group.[43] A peak at 9.70 ppm is due to the phenolic —OH proton resonance.[31] A very weak broad peak at 11.94

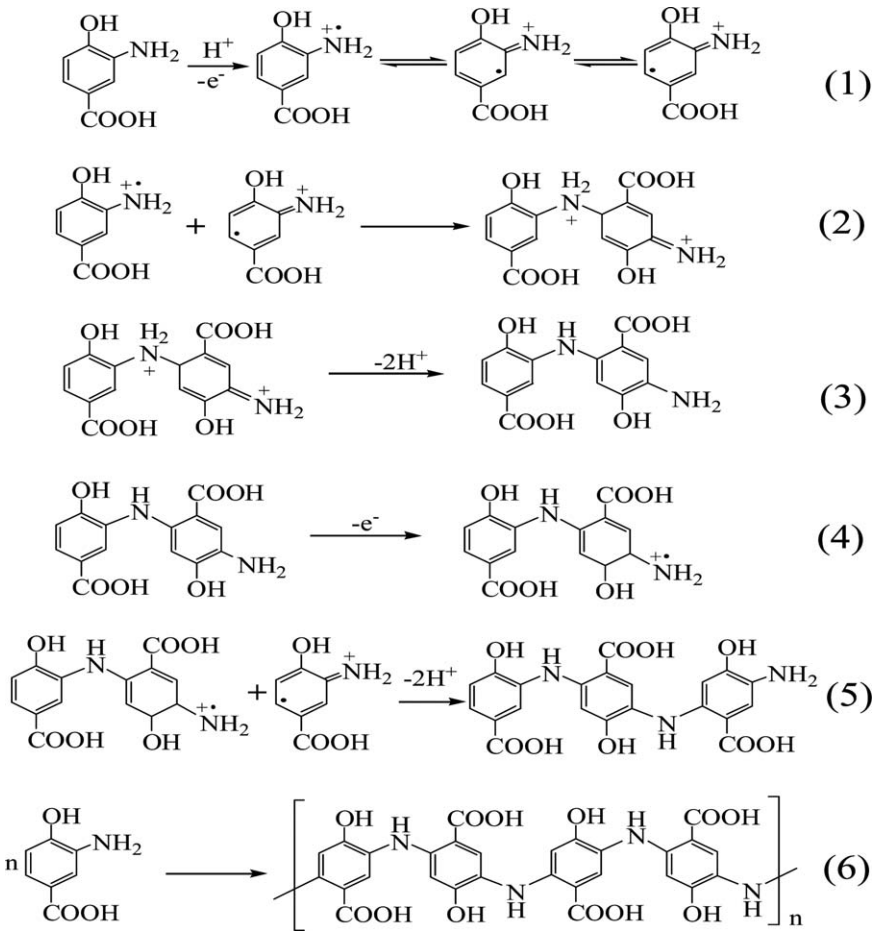

Scheme 1. Electrochemical polymerization mechanism of AHBA.

ppm is attributed to the —COOH proton resonance. Figure 9(B) displays the ^{1}H NMR spectrum of PAHBA. As can be seen in Figure 9(B), there is a set of sharp triplet peaks at 6.972, 7.057, and 7.142 ppm with almost equal intensity and a coupling constant of $^{1}J_{NH}$ 51.1 Hz. The triplet peaks are attributed to the free-radical NH proton resonance of PAHBA, similar to that of polyanline.[42,44,45] The two peaks at 6.70 and 7.23 ppm in the monomer spectrum also appear in the polymer spectrum, but they become very weak. These results indicate that aromatic protons on the *ortho* positions of the —OH group and the —NH_2 group of the monomer still remain in the AHBA units of the polymer chain. However, the two monomer peaks at 4.90 and 7.10 ppm disappear in the polymer spectrum, indicating that the *para*-position carbon of the —NH_2 group of one AHBA molecule was coupled to the nitrogen of another AHBA molecule to form a polyaniline-like chain. In addition, the two monomer peaks attributed to the —OH group and —COOH group appear at 10.96 and 9.59 ppm, but they become much weaker in the polymer spectrum than in the monomer spectrum. This demonstrates that the —OH group and —COOH group exist in the AHBA unit of the polymer chain. From the ^{1}H NMR analysis, it can be concluded that PAHBA has a polyaniline-like head-to-tail coupled structure with an —OH group and a —COOH group in each AHBA unit.

XPS Spectra

The XPS spectra of the polymer were measured. The high-resolution XPS spectrum of C 1s is presented in Figure 10(A). The binding energy, area of the peak, and the percentage of carbon atoms with different binding energies are listed in Table I. The C 1s core level spectrum involved four peaks at 291.4, 288.7, 286.3, and284.7 eV for the PAHBA. The weak and broad peaks at 291.4 eV is a C1s shake-up satellite peak due to a π–π^{*} transition in aromatic molecules.[46] The other three peaks indicate that there are at least three different carbon atoms with different electronic states. The peak at 288.7 eV is attributed to the carboxylic (—COOH) groups in AHBA units, since the carbon atom is attached to two electronegative oxygen atoms *via* both a double bond (C═O) and a single bond(C—OH), i.e., the chemical environment of the C atom is different from those of other C atoms. The O atoms play a role in decreasing the shielding of the positive nuclear charges of C 1s by outer electrons. Thus, the effective attractive force of the nucleus with regard to the core electrons of C 1s is increased, i.e., its binding energy should be higher than those of other carbon atoms in the polymer. In addition, oxygen is more electronegative than nitrogen, and the binding energy of the carbon attached to oxygen is somewhat larger than that of the carbon attached to nitrogen. As a result, the peak at 286.3 eV can be assigned to the aromatic C—OH, C—N, and/or C═N bonds, while the

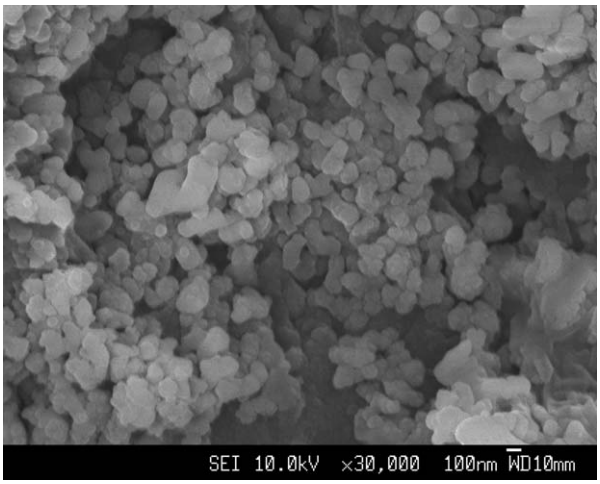

Figure 11. SEM image of PAHBA film electrodeposited on GC electrode.

most intense peak at 284.7 eV is attributed to the C—C or C—H bonds in AHBA units of the polymer. The calculated values of the carbon atom ratio based on the assuming form are also listed in Table I.

The high-resolution XPS spectrum of O 1s with two peaks is given in Figure 10(B). The first peak at 533.5 eV is attributed to the —OH group of phenolic rings[47] and carboxylic acid groups[48] and adsorbed H_2O,[47,49] and the second one at 531.5 eV is ascribed to the —C═O group of quinonic[47] and/or carboxylic acid[48] groups. These results demonstrate that the —OH and —COOH groups exist in the polymer chain.

Figure 10(C) shows the high-resolution XPS spectrum of N 1s. Two peaks appear at 401.5 and 399.9 eV, respectively. The first peak ascribed to the $—NH_2^+—$ group, and the second one is due to the —NH— group.[49] The doping ratio obtained ($—NH_2^+—/N_{Total}$) is 0.19. This is attributed to the ionized carboxylic acid ($—COO^-$) groups of the polymer.

Polymerization Mechanism

Based on the results of the PAHBA spectra and the previously described behavior of aniline,[50] *o*-aminophenol,[30] and 5-aminosalicylic acid,[51,52] it is reasonable to assume that the electrochemical polymerization of AHBA involves the processes
S1 outlined in Scheme 1. The initial step in the polymerization is that an AHBA molecule is oxidized to a radical cation on the working electrode (eq. 1). Two AHBA radical cations, mainly *N*- and *pare*-forms, are coupled to form a dimer cation (eq. 2), and then the dimer cation loses two protons to form a dimer (eq. 3). The dimer is oxidized to form a dimer radical cation (eq. 4), which further reacts with one AHBA radical to yield a trimer (eq. 5). As the reactions proceed, a polymer is formed finally (eq. 6). As can be seen in eq. (6) in Scheme 1, the proposed chemical structure of PAHBA is a leucoemeraldine base form. This is due to that the PAHBA film is reduced in the solution at the applied potential at −0.20 V which is the terminal potential during the electrochemical polymerization. Moreover, the color of the PAHBA film obtained here is similar to that of the polyaniline leucoemeraldine base form. However, it is different from that of the green PAHBA emeraldine base form deposited on platinum substrate in 1 M HCl at a constant potential of −1.50 V.[26]

SEM of the Polymer

Figure 11 is the SEM image of the PAHBA film electrodeposited on GC electrode, which shows well-dispersed spherical nanoparticles with an average diameter of 80–140 nm. This is due to that the low conductivity of PAHBA is unfavorable for the polymerization of AHBA on the polymer chains. The polymer chain radicals are first formed on the naked working electrode surface in the early stages of electrochemical polymerization. Then, polymer chain radical reacts very rapidly with the phenolic hydroxyl group of AHBA monomer in the solution. This leads to the formation of a molecule with a polar group, which is similar to surfactants. Based on the shaping theory, when the size of a molecule with a polar group approaches the proportion of a spherical particle morphology, it tends to aggregate spherical particles so as to minimize the surface.[18]

CONCLUSIONS

The PAHBA films were successfully fabricated via cyclic voltammetry. The polymer shows good electrochemical activity from a 0.50 M H_2SO_4 solution to a strongly basic solution with pH 12.0 in a wider potential range, which proves that the pH dependence of the polymer has been improved significantly as compared with polyaniline. This is due to each monomer unit with two pH functional groups of —OH and —COOH in the polymer chain, which work corporately in adjusting pH value in the bulk solution. SEM results show that the polymer film is assembled with spherical nanoparticles. Based on the results of the UV–visible, FTIR, and ^1H NMR spectra, a possible chemical structure of the resulting polymer is proposed here, i.e., the polymer chain was formed *via* the phenyl-*N*-phenyl bonds, similar to that of the unsubstituted polyaniline. However, the electropolymerization mechanisms of the resulting polymer are rather complicated, thus a further study on them is required. In addition, the PAHBA nanoparticles are able to offer a large surface area of active sites for the electrocatalytic reactions, and thus is a new promising electrode material for electroanalysis such as electochemical sensors and biosensors. Its applications are also to be investigated in detail.

ACKNOWLEDGMENTS

We acknowledge funding by the Natural Science Foundation of Jiangsu Province, China under Grant No. BK2012699, the Social Development Foundation of Zhenjiang City, Jiangsu Province, China under Grant No. SH2011016, and the Scientific Research Foundation for the Returned Overseas Chinese Scholars, State Education Ministry, China.

REFERENCES

1. Chiang, C. K.; Fincher, C. R.; Park, Y. W.; Heeger, A. J.; Shirakawa, H.; Louis, E. J.; Gau, S. C.; MacDiarmid, A. G. *Phys. Rev. Lett.* **1977**, *39*, 1098.
2. Long, Y. Z.; Li, M. M.; Gu, C. Z.; Wan, M. X.; Duvail, J . L.; Liu, Z. W.; Fan, Z. Y. *Prog. Polym. Sci.* **2011**, *36*, 1415.

3. Das, T. K.; Prusty, S. *Polym. Plast. Technol.* **2012**, *51*, 1487.
4. Nguyen, M. T.; Kasai, P.; Miller, J. L.; Diaz, A. F. *Macromolecules* **1994**, *27*, 3625.
5. Liao, Y. Z.; Strong, V.; Chian, W.; Wang, X.; Li, X. G.; Kaner, R. B. *Macromolecules* **2012**, *45*, 1570.
6. Li, X. W.; Zhang, H.; Wang, G. C.; Jiang, Z. H. *J. Mater. Chem.* **2010**, *20*, 10598.
7. Zhang, X.; Zhu, J. H.; Haldolaarachchige, N.; Ryu, J.; Young, D. P.; Wei, S. Y.; Guo, Z. H. *Polymer* **2012**, *53*, 2109.
8. Pan, L. J.; Qiu, H.; Dou, C. M.; Li, Y.; Pu, L.; Xu, J. B.; Shi, Y. *Int. J. Mol. Sci.* **2010**, *11*, 2636.
9. Tran, H. D.; D'Arcy, J. M.; Wang, Y.; Beltramo, P. J.; Strong, V. A.; Kaner, R. B. *J. Mater. Chem.* **2011**, *21*, 3534.
10. Luo, J.; Zhou, Q.; Sun, J.; Jiang, J.; Zhou, X.; Zhang, H.; Liu, X. *J. Polym. Sci. Part A: Polym. Chem.* **2012**, *50*, 4037.
11. Kumar, S.; Singh, V.; Aggarwal, S.; Manda, U. K. *Colloid. Polym. Sci.* **2009**, *287*, 1107.
12. Virji, S.; Huang, J. X.; Kaner, R. B.; Weiller, B. H. *Nano Lett.* **2004**, *4*, 491.
13. Huang, J. X.; Virji, S.; Weiller, B. H.; Kaner, R. B. *J. Am. Chem. Soc.* **2003**, *125*, 314.
14. MacDiarmid, A. G.; Jones, W. E.; Norris, I. D.; Gao, J.; Johnson, A. T.; Pinto, N. J.; Hone, J.; Han, B.; Ko, F. K.; Okuzaki, H.; Llaguno, M. *Synth. Met.* **2001**, *119*, 27.
15. Gao, C.; Ai, M.; Li, X.; Xu, Z. *J. Polym. Sci. Part A: Polym. Chem.* **2011**, *49*, 2173.
16. Huang, J. X.; Kaner, R. B. *Chem. Commun.* **2006**, *28*, 367.
17. Liang, L.; Liu, J.; Windisch, C. F.; Exarhos, G. J.; Lin, Y. H. *Angew. Chem. Int. Ed.* **2002**, *41*, 3665.
18. Tran, H. D.; Kaner, R. B. *Chem. Commun.* **2006**, *28*, 3915.
19. Chen, C. X.; Sun, C.; Gao, Y. H. *J. Macromol. Sci. A* **2008**, *45*, 974.
20. Chevalier, J. W.; Bergeron, J. Y.; Dao, L. H. *Macromolecules* **1992**, *25*, 3325.
21. Cattarin, S.; Doubova, L.; Mengoli, G.; Zotti, G. *Electrochim. Acta* **1988**, *33*,1077.
22. Mu, S. L.; Lu, Y. L.; Qian, B. D. *Acta Phys. Chim. Sin.* **1989**, *5*, 207.
23. Wei, Y.; Focke, W. W.; Wnek, G. E.; Ray, A.; MacDiarmid, A. G. *J. Phys. Chem.* **1989**, *93*, 495.
24. Li, X. G.; Huang, M. R.; Duan, W.; Yang, Y. L. *Chem. Rev.* **2002**, *102*, 2925.
25. Chen, C. X.; Ding, G. Q.; Zhou, D.; Lu, X. H. *Electrochim. Acta* **2013**, *97*, 112.
26. Kan, K.; Yamamoto, H.; Kaneko, D.; Tateyama, S.; Kaneko, T. *Pure Appl. Chem.* **2014**, *86*, 685.
27. Barbero, C.; Silber, J. J.; Sereno, L. *J. Electroanal. Chem.* **1989**, *263*, 333.
28. Zhang, A. Q.; Cui, C. Q.; Chen, Y. Z.; Lee, J. Y. *J. Electroanal. Chem.* **1997**, *373*,115.
29. Gonçalves, D.; Faria, R. C.; Yonashiro, M.; Bulhões, L. O. S. *J. Electroanal. Chem.* **2000**, *487*, 90.
30. Carbone, M. E.; Ciriello, R.; Granafei, S.; Guerrieri, A.; Salvi, A. M. *Electrochim. Acta* **2014**, *144*, 174.
31. Mu, S. L. *Synth. Met.* **2011**, *161*, 1306.
32. Mu, S. L. *Synth. Met.* **2004**, *143*, 259.
33. Geniès, E. M.; Boyle, A.; Lapkowski, M.; Tsintavis, C. *Synth. Met.* **1990**, *36*, 139.
34. Yin, W.; Ruckenstein, E. *Synth. Met.* **2000**, *108*, 39.
35. Yamamoto, K.; Yamada, M.; Nishiumi, T. *Polym. Adv. Technol.* **2000**, *11*, 710.
36. Eo, S. M.; Oh, S. J.; Tan, L. S.; Baek, J. B. *Eur. Polym. J.* **2008**, *44*, 1603.
37. Griffith, W. P.; Koh, T. Y. *Spectrochim. Acta A* **1995**, *51*, 253.
38. Soliman, U. A.; Hassan, A. M.; Mohamed, T. A. *Spectrochim. Acta A* **2007**, *68*, 688.
39. Panicker, C. Y.; Varghese, H. T.; John, A.; Philip, D.; Istvan, K.; Keresztury, G. *Spectrochim. Acta A* **2002**, *58*, 281.
40. Akkaya, Y.; Akyuz, S. *Vib. Spectros.* **2006**, *42*, 292.
41. Trchová, M.; Morávková, Z.; Bláha, M.; Stejskal, J. *Electrochim. Acta* **2014**, *122*, 28.
42. Mu, S. L. *J. Phys. Chem. B* **2008**, *112*, 6344.
43. Spectral Database for Organic Compounds. http://sdbs.db.aist.go.jp/sdbs/cgi-bin/direct_frame_disp.cgi?sdbsno=5680.
44. Wang, X.; Sun, T.; Wang, C.; Wang, C.; Zhang, W.; Wei, Y. *Macromol. Chem. Phys.* **2010**, *211*, 1814.
45. Rana, U.; Mondal, S.; Sannigrahi, J.; Sukul, P. K.; Amin, M. A.; Majumdar, S.; Malik, S. *J. Mater. Chem. C* **2014**, *2*, 3382.
46. Schröder, K.; Meyer-Plath, A.; Keller, D.; Ohl, A. *Plasmas. Polym.* **2002**, *7*, 103.
47. Carbone, M. E.; Ciriello, R.; Guerrieri, A.; Salvi, A. M. *Int. J. Electrochem. Sci.* **2014**, *9*, 2047.
48. Losito, I.; Malitesta, C.; De Bari, I.; Calvano, C. D. *Thin Solid Films* **2005**, *473*, 104.
49. Monkman, A. P.; Stevens, G. C.; Bloor, D. *J. Phys. D: Appl. Phys.* **1991**, *24*, 738.
50. Wallace, G. G.; Spinks, G. M.; Kane-Maguire, L. A. P; Teasdale, P. R. Conductive Electroactive Polymers: Intelligent Polymer Systems, 3rd ed.; CRC Press: Boca Raton, **2009**; p 138.
51. Palsmeier, R. K.; Radzik, D. M.; Lunte, C. E. *Pharm. Res.* **1992**, *9*, 933.
52. Eriksson, A.; Nyholm, L. *Electroanalysis* **1998**, *10*, 198.